JOURNAL OF AIRCRAFT
Vol. 32, No. 2, March–April 1995

Numerical Study of a Supersonic Open Cavity Flow and Pressure Oscillation Control

Yih Nen Jeng* and Uon Jan Payne†
National Cheng Kung University, Tainan, Taiwan, Republic of China

Numerical experiments were performed to study the flow structure and suppression of pressure oscillation in the $M_\infty = 2.5$ supersonic open cavity flow problem. Numerical results show that the large pressure variation within the cavity induced by the shear layer's wavy shape produces new vortices not found in situations where $M_\infty < 2.5$. The proposed suppression device imposes mass transfer on the cavity's aft bulkhead. The proposal is tested by replacing one of the cavity walls with a porous wall and adjoining vent chamber. Constant porosity and uniform vent-chamber pressure are assumed. Replacing the aft bulkhead with a porous wall/vent chamber combination provides the most effective suppression of pressure fluctuation, even with a porosity value as small as 0.1 for vent-chamber pressure ranging from p_∞ to $1.5p_\infty$. Mass transfer at the cavity floor and forward bulkhead are also examined, but they are found to be less effective.

Nomenclature

D, L = depth and length of the cavity, respectively
F, G = inviscid fluxes along x and y directions, respectively
F_v, G_v = viscous fluxes along x and y directions, respectively
J = $1/J$ is the area of the quadrilateral cell
K = permeability of the porous wall
M = Mach number
Pr = Prandtl number
p = pressure
q = acoustic sound reference level of 2×10^{-5} Pa
t = time
t_c = u_∞/D, characteristic time
U = $1/J[\rho, \rho u, \rho v, e]^T$, dependent variables
u, v = velocity components along x and y directions, respectively
x, y = Cartesian coordinates
y^+ = dimensionless distance measured from wall in turbulent boundary layer
γ = specific weight of fluid
Δx = thickness of porous wall
ε = infinitesimal constant to avoid dividing by zero
μ = dynamic viscosity
ξ, η = curvilinear coordinates
ρ = fluid density
σ = geometric porosity factor

Subscripts

c = vent-champer properties
j, k = grid indices on computational domain
t = turbulent properties
w = wall properties
∞ = freestream value

Superscripts

n = time steps
$\sim$ = numerical value

Received Oct. 6, 1993; revision received Feb. 15, 1994; accepted for publication July 5, 1994.

*Associate Professor, Institute of Aeronautics and Astronautics. Member AIAA.
†Graduate Student.

I. Introduction

HIGH-SPEED flow over an open cavity produces a complex oscillatory flowfield that is not only of fundamental physical interest, but is also of significant practical concern. Cavities occur in many aerodynamic configurations, such as weapon bays in bombers and wheel wells on aircraft. The resulting large pressure fluctuations generate loud noise and may damage the cavity structure and sensitive instruments within the cavity.[1-7] In a recent study of controlled store separation from a cavity, Atwood[8] found that the store load experienced the maximum rms disturbance level as the store was traversing the free shear layer. He also found that the store loads from the controlled simulation generally possess a higher rms disturbance level as compared to the uncontrolled simulation. Suppression of violent pressure oscillation is thus an important aerodynamic issue.

Rossiter[9] first proposed a feedback mechanism between shedding vortices and acoustic waves to explain the self-sustained cavity flow oscillation. Heller and Bliss[10] improved the Rossiter empirical relation that predicted the dominant frequencies of oscillation. Hankey and Shang[11] improved upon Rossiter's empirical relation by employing linear stability analysis to the problem of cavity shear layer instability. For the subsequent important works, readers are urged to access Refs. 1–7.

Many control techniques have been tested to alleviate undesired cavity flow fluctuation. Conventional suppression techniques have been surveyed by Rockwell et al.,[1] but most of the successful cavity flow suppression techniques can be identified by whether they affect the flow phenomena described in the documented physical models.[1,6,10,12,13] Active pneumatic control has been experimentally studied in an attempt to suppress flow oscillation.[14,15] Recently, Chokani and Kim[16,17] used a porous surface with a vent chamber beneath the floor of the cavity to show that a venting system can also be effective in suppressing pressure fluctuations within the cavity. The present study proposes another method based on the porous plate idea of Chokani and Kim.

Borland[18] first solved the two-dimensional Euler equations for high subsonic flow over an open cavity. Hangkey and Shang's simulation[19] of supersonic open cavity flow via two-dimensional Navier-Stokes equations prompted a number of numerical studies.[20-29] Because of significant advances in computer hardware, two- and three-dimensional numerical simulation of the controlled store separation problem[8] has become practical. Rizzetta[23] obtained the harmonic frequen-

cies of a three-dimensional open cavity using two- and three-dimensional Navier-Stokes equations. He concluded that the fundamental behavior of unsteady phenomena in cavities is two dimensional. The experimental and numerical investigations of Zhang and Edwards[24,25] also support the validity of the two-dimensional analysis. In order to save computer resources, a two-dimensional model is employed here.

The main concern of this article is to numerically explore the possibility of reducing pressure fluctuation by means of replacing a solid wall in an open cavity with a porous wall and adjoining vent chamber. The numerical scheme is a third-order upwind total variation diminishing (TVD) scheme based on the Coakley flux difference splitting method,[30] and employs a modified version[31,32] of Leonard and Niknaf's[33] extremum corrector. Because of the large number of parameters determining the flow structure, as well as for the sake of comparison, this study will concentrate on the flow conditions and the geometry of Zhang and Edwards' works,[24,25] in which the $M_\infty = 2.5$ supersonic open cavity flow problem was experimentally and numerically studied.

II. Numerical Method

For open-cavity flow, the conservation form of the nondimensional unsteady, compressible, Reynolds-averaged, complete Navier-Stokes equations are descretized in the following fully implicit form:

$$\tilde{U}^{n+1}_{j,k} + \Delta t\{\tilde{F}^{n+1}_{j+1/2,k} - \tilde{F}^{n+1}_{j-1/2,k} - (1/Re)[(\tilde{F}_v)^{n+1}_{j+1/2,k} - (\tilde{F}_v)^{n+1}_{j-1/2,k}]\} + \Delta t\{\tilde{G}^{n+1}_{j,k+1/2} - \tilde{G}^{n+1}_{j,k-1/2} - (1/Re)[(\tilde{G}_v)^{n+1}_{j,k+1/2} - (\tilde{G}_v)^{n+1}_{j,k-1/2}]\} = \tilde{U}^n_{j,k} \quad (1)$$

A TVD scheme[13,31,32] similar to the maximum-compressive-factor third-order upwind scheme of Chakravarthy and Osher,[35] which applies the Coakley upwind difference splitting[30] and approximate Riemann solver[34] along the ξ and η directions separately, is employed to the convective terms. Because TVD schemes exhibit clipping across extreme points, the TVD limiter function was not switched around a physical extremum.[31-33] The resulting algebraic equations are iteratively solved in terms of the Newton-Raphson method and the alternating direction implicit (ADI) factorization method of Yee and Harten.[37-39]

For calculating turbulent flow, the molecular transport coefficients are modified as

$$\mu = \mu + \mu_t \qquad \frac{\mu}{Pr} = \frac{\mu}{Pr} + \frac{\mu_t}{Pr_t} \quad (2)$$

where Pr and Pr_t are 0.72 and 0.9, respectively. The turbulent viscosity is estimated in terms of the Baldwin and Lomax algebraic two-layer formulation[36] with the modification for the cavity flow[20,22]

$$\mu_t = \frac{(\mu_t/y^+)_{fb} + (\mu_t/y^+)_f + (\mu_t/y^+)_{ab}}{[(1/y^+)^2_{fb} + (1/y^+)^2_f + (1/y^+)^2_{ab}]^{1/2}} \quad (3)$$

where the subscripts fb, f, and ab denote variables evaluated with respect to the forward bulkhead, floor, and aft bulkhead, respectively.

Supersonic open cavity flow, with an inflow Mach number of 2.5, was first examined by Zhang[24,25] for a cavity with a length-to-depth ratio L/D of 3.0. According to Hankey and Shang's[11] linear stability analysis, a freestream Mach number larger than 2.5 may not induce Rayleigh instability. Therefore, this setup provides a suitable test of the employed TVD scheme's modeling ability. The grid system includes two zones (102 × 42 and 60 × 30 points), depicted by the nonuniform mesh systems in Fig. 1. The overall extent of the domain is

$$-1.35 \le x/D \le 6.0, \qquad -1.0 \le y/L \le 4.0 \quad (4)$$

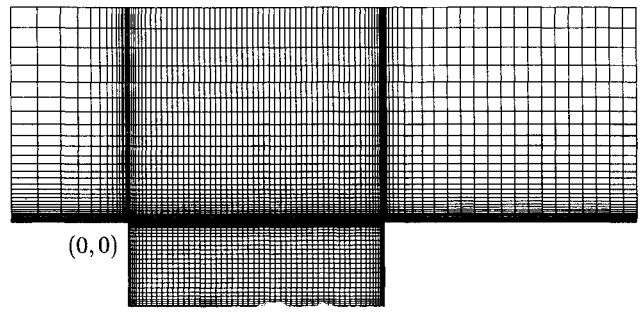

Fig. 1 Computation domain and grid distribution.

In the upstream boundary layer above the flat plate, the first mesh is located at $y^+ = 8$ ($y^+ = yu^*/\nu_w$, $u^* = \sqrt{\tau_w/\rho_w}$), which is based on the Musker velocity profile of the turbulent boundary layer.[40] This arrangement results in 22 grid points within the boundary layer.

On all solid boundaries, we invoke nonslip and adiabatic conditions and the condition of zero-normal-gradient of pressure. To simulate the flow through the porous surface, the normal wall velocity over the porous surface is approximated by the linear form of the Darcy pressure-velocity law[16,17]

$$v_w = \sigma/\rho_\infty u_\infty (p_c - p_w) \quad (5)$$

where $\sigma = \gamma K/\mu \Delta x \rho_\infty u_\infty$ is the parameter for geometric porosity. For convenience, the porosity and vent-chamber pressure p_c are assumed to be constant.

A turbulent boundary-layer solution over a corresponding flat plate, with an inflow Mach number of 2.5, Reynolds number of 4.5×10^5 (based on cavity depth), and a displacement boundary thickness of $\delta/D = 0.3$, is used to approximate the fixed upstream inflow conditions of Zhang's experiment. Other inflow conditions include a total pressure P_0 of 2319 mmHg, and a total temperature T_0 of 290 K. The downstream boundary conditions are given by a simple zeroth-order extrapolation from interior nodes. At the upper boundary, derivatives along instantaneous Mach lines are set to zero.[41]

The initial conditions are taken as the flat plate solution at all the grid points above the cavity mouth. To employ the algebraic turbulence model within the cavity, very small values are assigned to the u and v velocity components, whereas other variables take on the wall values. Six subiterations are employed to reduce the l_2 residual by approximately three orders of magnitude such that the CPU time per iteration is about 9.93 s on an HP720 workstation. During the computations, a constant time step Δt of $0.01tc$ is used, which corresponds to a maximum Courant number of 5.528. Starting from the initial profiles, the flowfield is integrated for $40t_c$ to purge the initial transient period. Time-dependent data is then collected from the resulting self-sustaining flowfield over the next 200 characteristic time units.

To simulate the predominantly two-dimensional oscillation behavior of cavity flow, the computed power spectrum density (PSD) in the frequency domain is compared with Zhang's experimental results.[24,25,42] The PSD is defined as

$$\text{PSD} = 10 \log_{10}[|SP(\omega)|/2\omega] \quad (6)$$

where $SP(\omega)$ represents the auto-spectral density function calculated from the fluctuating component of the pressure, and ω represents the circular frequency.

III. Numerical Results and Discussion

To validate the computational code, numerical solution of the open cavity flow without control is first obtained. The PSD values shown in Fig. 2 represent measurements at $x/D = 0.333$ and 2.333 on the cavity floor. The top and bottom

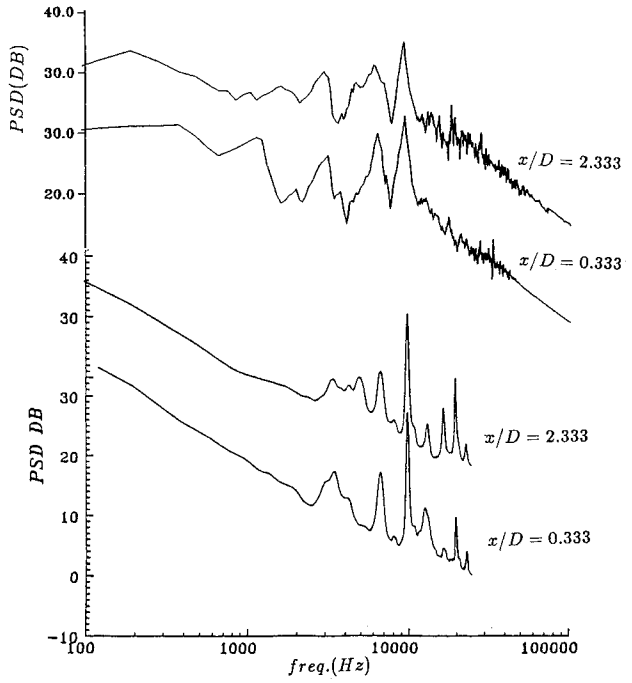

Fig. 2 Power spectral density inside cavity ($M_\infty = 2.5$, $L/D = 3$, $Re_D = 450{,}000$); top pair, the present numerical result; bottom pair, experimental data of Ref. 42.

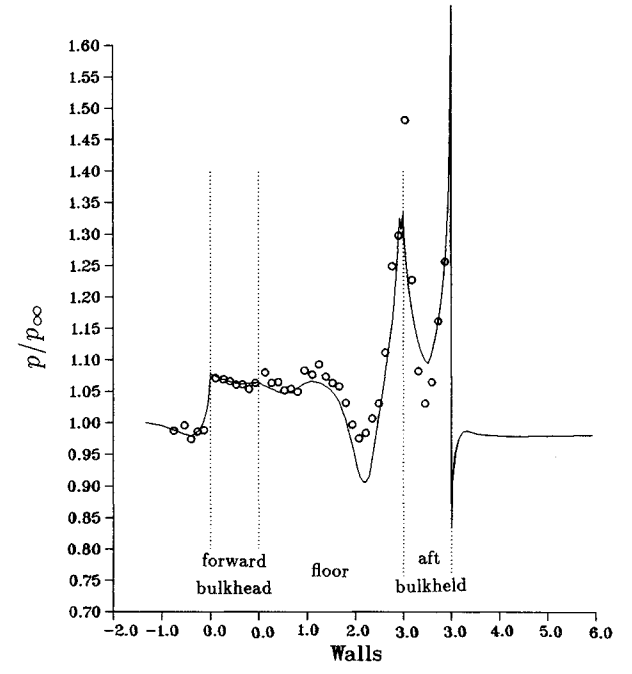

Fig. 3 Mean static pressure distribution on walls: open circle, experimental data of Ref. 42; solid line, numerical result.

pairs of values in this figure represent, respectively, the results of the numerical solution and the corresponding experimental data. Numerically predicted mean static pressure distribution along the cavity walls (e.g., forward bulkhead, floor, and aft bulkhead) are shown as solid lines in Fig. 3. For comparison, the experimental data of Zhang and Edwards[24,25,42] are marked with open circles. The discrepancies between the numerical and experimental data are believed to be caused by imperfect turbulent modeling, insufficent grid resolution, and three-dimensional mechanisms. Nevertheless, the power spectrum's main characteristics, especially the first two dominant frequencies, are numerically captured. Although the present

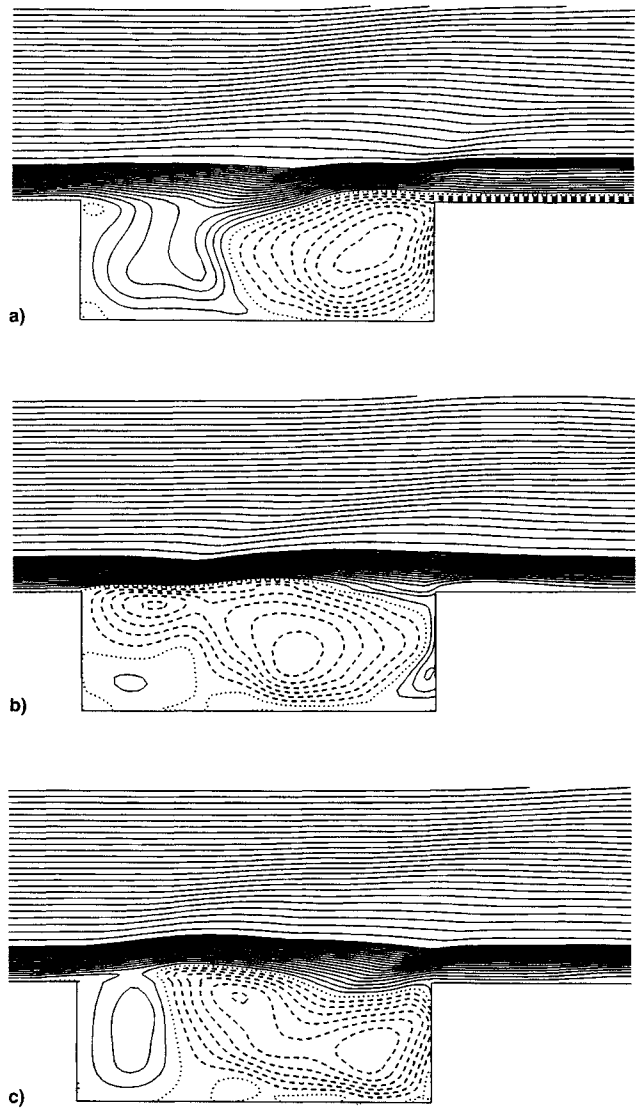

Fig. 4 Instantaneous streamlines in sequence of the noncontrolled cavity flow: t = a) 73.8, b) 75.9, and c) $78.3t_c$.

scheme cannot give an accurate prediction of the mean static pressure, it can, however, resolve the local minimum characteristic and give a qualitative indication of other flow trends.

The first three dominant frequencies predictions by the present work are 3129, 6352, and 9387 Hz, the prediction from modified Rossiter's formula[10] are 3078, 6855, and 10,633 Hz, and experimental data[24,25] are 3230, 6335, and 9636 Hz, respectively. Obviously, the modified Rossiter model is less accurate than the present results. According to Hankey and Shang's linear stability analysis,[11] a freestream Mach number larger than 2.5 may not induce Rayleigh instability of the free shear layer. Therefore, we will examine the flow structure to see why the dominant frequencies cannot be accurately predicted by the classical model.

After examining the video tape of the numerical solution, a sequence of representative instantaneous streamline (Figs. 4a–4c) and pressure contours (Figs. 5a–5c) are chosen. For the sake of clarity, solid, dashed, and dotted lines are employed within the cavity, representing counterclockwise rotating streamlines, clockwise rotating streamlines, and the zero value line of the stream function, respectively. The latter correspond to the divided streamlines between the counter-rotated vortices.

A careful comparison of the low-speed model[9–11,13] to the flow structure of the present model, reveals many similar

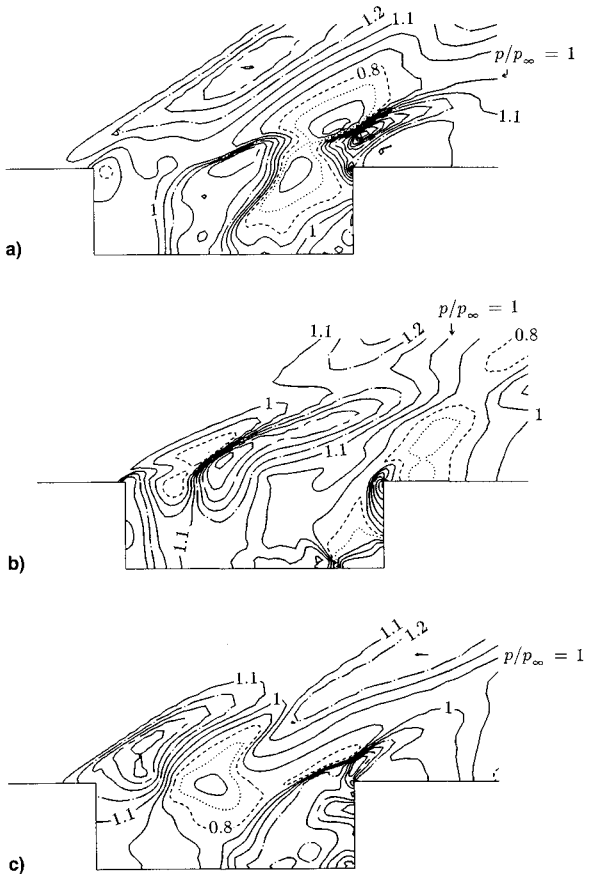

Fig. 5 Instantaneous pressure contours in sequence of the noncontrolled cavity flow, $\Delta p/p_\infty = 0.1$: t = a) 73.8, b) 75.9, and c) $78.3t_c$.

features: 1) that vortices are always present within the cavity; 2) a large vortex periodically oscillates, standing near the aft bulkhead (Fig. 4a); 3) at times this vortex extracts fluid from the cavity (Fig. 4a), while at other times, it merges with the leading-edge vortex (Fig. 4b and 4c); 4) both compression and expansion waves occur in the external flow (Figs. 5a–5c); and 5) waves initiated at the aft bulkhead (Fig. 5b) collide with the forward bulkhead (Fig. 5b), and induce the free shear layer's deflection at the leading-edge corner of the cavity. Note that the large vortex of items 2 and 3 induces the local minimum of the mean static pressure on the floor. On the other hand, there are many phenomena not found in the low-speed case. First, the shape of the free shear layer principally dictates the sequential appearance of high-low pressure zones within the cavity. The difference between high- and low-pressure peaks is very large ($p \sim 0.5 - 1.5p_\infty$) over a short distance, so that the pressure field is an important factor in determining the vortex structure. The pressure variation for those cases in which $M_\infty < 2.5$ is, however, not large enough to dominate oscillatory vortex structure. Second, instead of directly inducing the leading-edge vortice, waves that collide with the forward bulkhead enhance the lower left corner counter-clockwise rotated (CCW) vortice (Fig. 4c). The CCW vortex becomes a U-shape structure and then triggles a leading-edge vortex (Fig. 4a). Third, at the aft bulkhead, local low-pressure zones and vortex merging impulsively suck fluid into the cavity (Figs. 4b and 5b).

It is not clear whether these differences can be attributed to differences of the linear stability characteristics in the free shear layer. It seems that further studies on the linear and nonlinear stability are necessary. We next investigate the suppression of pressure fluctuation within the cavity.

In their passive venting study, Kim and Chokani[16,17] used a geometric porosity factor of 0.607 to simulate the 11.2% porosity of the porous cavity floor. Wilcox[43] used a porous-

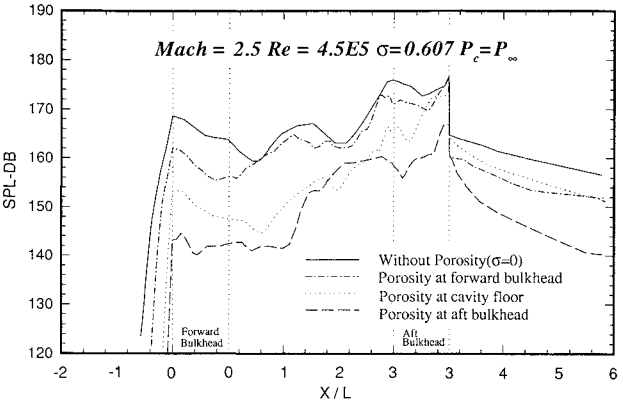

Fig. 6 Comparison of sound pressure level at different locations with/without the porous wall controlled with $p_c = p_\infty$ and $\sigma = 0.607$.

floor to convert the closed cavity flow to an open flow and found that the porosity near the cavity midlength did not significantly affect the venting process. In view of his conclusion, it is interesting to examine whether a porosity factor as small as 0.1 can suppress the pressure oscillation in the cavity. Accordingly, in this study four porosity factors are examined: 0.1, 0.267, 0.433, and 0.607.

The average mean static pressure along the aft bulkhead (see Fig. 3) is $1.21p_\infty$. If the vent-chamber pressure, averaged over time, is less than this value, air must be extracted from it by adding a pump or using a channel to connect the vent chamber to the freestream at some location far downstream. The first representative case, then, is $p_c = p_\infty$ with $\sigma = 0.607$.

To get quantitative data, the oscillatory pressure distribution along the cavity's forward bulkhead, floor, and aft bulkhead is redefined to be overall sound pressure level (SPL) in decibels (dB), which can be expressed as[23]

$$\text{SPL} = 10 \log_{10}\left(\frac{\overline{p'^2}}{q^2}\right) \tag{7}$$

$$\overline{p'^2} = \left(\frac{1}{t_f - t_i}\right)\int_{t_i}^{t_f} (p - \bar{p})^2 \, dt \tag{8}$$

The sampling duration of the SPL calculation in Eq. (8) is from t_i ($=70t_c$) to t_f ($=100t_c$). The SPL distributions in Fig. 6 ($\sigma = 0.607$) are shown in sequence along the horizontal axis starting from the left—first the upstream flat plate; then the forward bulkhead, floor, and aft bulkhead; and finally the downstream flat plate. The furthest limits of each wall's distribution is delineated by a dashed line.

An inspection of the figure reveals clearly that a porous aft bulkhead is more effective at suppressing pressure fluctuation than either a porous floor or forward wall. The porous rear wall provides the greatest reduction in SPL value for two reasons. First, mass exchange is greatest across the rear porous wall. Second, suppression of the initiation of the upstream propagating wave is more effective than attenuation of the wave either during its propagation or at the instance of impingement on the forward wall.

Figure 7 shows a sequence of representative instantaneous streamline contours resulting from the use of a porous wall at the aft bulkhead. Mass extraction and injection occur along the rear wall. Flow oscillation persists, but the figures show that the magnitude of shear layer vibration is so small that the main flow structure is much less violent than those shown in Figs. 4a–4c. In fact, the impinging point of the free shear layer on the wall is nearly steady. Moreover, the vortices shed from the leading-edge corner are so small in size that any resulting vortex-merging phenomena are nonviolent.

Next, the porosity and vent-chamber pressure are considered as parameters. The resulting SPL distributions for the

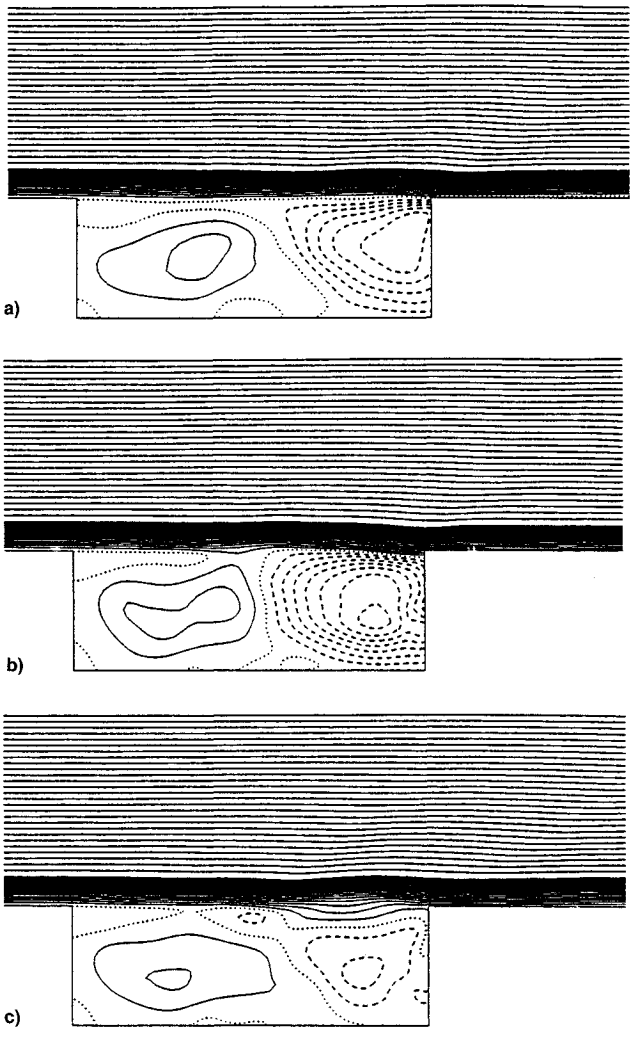

Fig. 7 Instantaneous streamlines in sequence after flow oscillations being suppressed, controlled with $p_c = p_\infty$ and $\sigma = 0.607$: t = a) $90.0t_c$, b) $91.8t_c$, and c) $93.6t_c$.

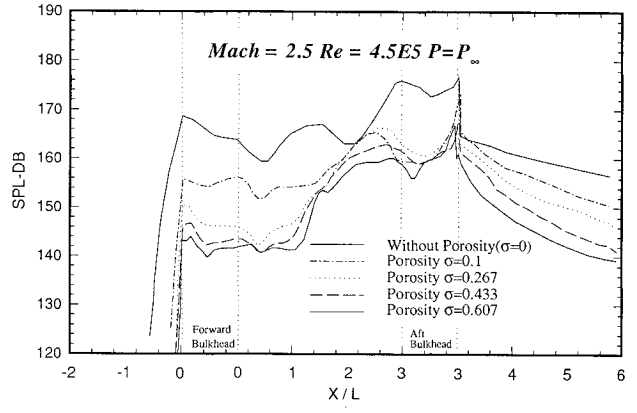

Fig. 8 Comparison of sound pressure level for different porous factors along the aft bulkhead, controlled with $p_c = p_\infty$.

case of $p_c = p_\infty$ are shown in Fig. 8, where a small porosity ($\sigma = 0.1$) significantly suppresses the high-pressure oscillation near the aft bulkhead (about a 10 dB reduction). The region next to the aft bulkhead is affected to a lesser extent, exhibiting only about a 5 dB reduction. An examination of Fig. 8 reveals that the greater the porosity, the greater the reduction in SPL.

Because the pressure within the vent chamber is assumed to be uniform, vent chamber pressure p_c should be expressed

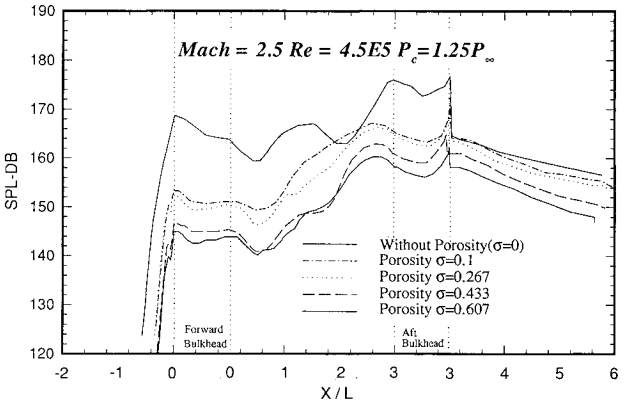

Fig. 9 Comparison of sound pressure level for different porous factors along the aft bulkhead, controlled with $p_c = 1.25p_\infty$.

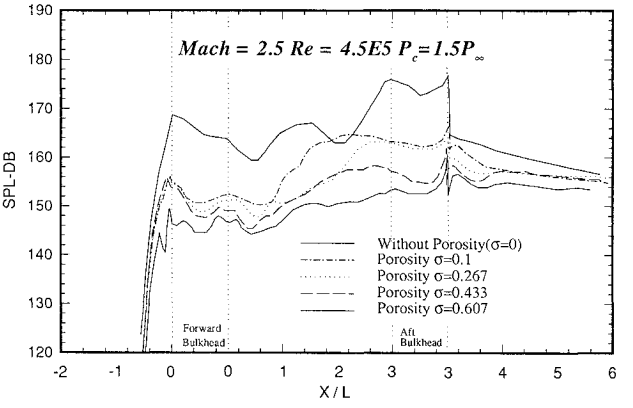

Fig. 10 Comparison of sound pressure level for different porous factors along the aft bulkhead, controlled with $p_c = 1.5p_\infty$.

as $p_c \geq p_\infty$; otherwise, an enormous vacuum pump would be needed to provide the necessary suction rate. On the other hand, if the vent-chamber pressure is much larger than the calculated mean pressure over the solid aft bulkhead ($= 1.21p_\infty$), a huge device would be required to pump air into the cavity. Therefore, this study considers two additional vent pressures: $p_c = 1.25p_\infty$ and $1.5p_\infty$.

Figure 9 shows the SPL distribution for $p_c = 1.25p_\infty$, whereas Fig. 10 shows the same distribution for $p_c = 1.50p_\infty$. In all cases, even with σ as small as 0.1, pressure oscillation on and around the forward and aft bulkheads is effectively suppressed. Wilcox[43] experimentally showed that the porous floor arrangement was very effective in modifying the cavity flowfield. Because his data also showed that the porosity near the cavity midlength did not significantly affect the venting process, he suggested that an array of tubes could be used to modify the cavity flowfield. Obviously, although the main concerns are different, the findings of the present study are in some sense similar to his conclusion.

A careful examination of Figs. 8–10 reveals that an increase in wall porosity corresponds to a greater reduction in SPL over the range $p_\infty \leq p_c \leq 1.5p_\infty$. For a fixed wall porosity, increasing vent-chamber pressure improves SPL reduction near the aft bulkhead, but has the opposite effect in the upstream portion of the cavity. The latter phenomenon occurs because the greater the vent-chamber pressure, the greater the amount of air injected into the cavity, thus increasing the pressure throughout. Small peaks in the SPL distributions at the upstream flat plate (see Figs. 9 and 10) are due to the upstream effect passing through the boundary layer.

In fact, the series of streamline contours in Fig. 11, e.g., show that the venting chamber (with $p_c \geq 1.25p_\infty$) frequently pumps fluid into the cavity. This pumped mass flows out of the cavity near the upper corner of the aft bulkhead, forming

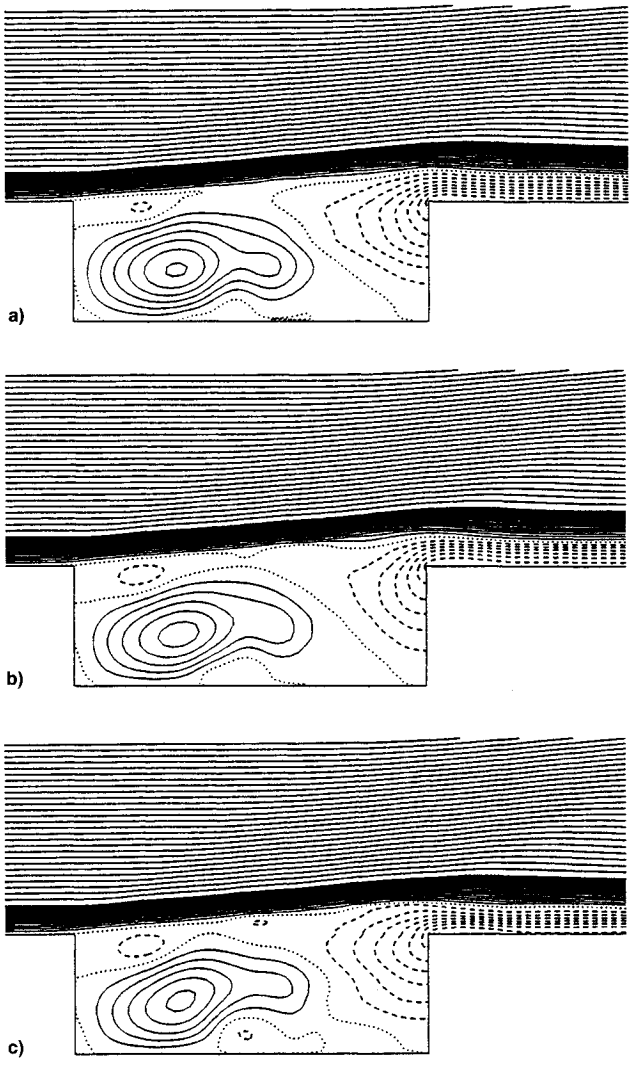

Fig. 11 Instantaneous streamlines in sequence after flow oscillations being suppressed, controlled with $p_c = 1.5p_\infty$ and $\sigma = 0.607$: t = a) $90.0t_c$, b) $91.8t_c$, and c) $93.6t_c$.

a fluid layer that significantly reduces the interaction between the free shear layer and the upper corner of the aft bulkhead. As a consequence, the pressure fluctuation is reduced even more when $p_c = p_\infty$. An inspection of the SPL distributions in Figs. 7–10 verifies this result.

In summary, placing a vent chamber behind a minimally porous wall located at the aft bulkhead effectively suppresses violent pressure fluctuations. Increasing the porosity results in an insignificant increase in the suppression effect. Pumping fluid into the cavity results in more effective SPL reduction than when the pump is not used. However, the addition of mass to the vent chamber (represented by $p_c = 1.50p_\infty$) requires adding energy to the pumping system. Extraction of mass from the cavity (represented by $p_c = p_\infty$) can be achieved by connecting the vent chamber through a channel to a downstream region of the flat plate. Although this setup may result in less SPL reduction when compared with the pumping system, it is more economical and should not be overlooked for future studies.

IV. Conclusions

For the present supersonic open cavity flow with $M_\infty = 2.5$, numerical investigation shows that the flow structure was somewhat different from that described by the classical low-speed model. The presence of the CCW vortices and U-shaped structure play important roles in inducing pressure oscillation. To suppress pressure fluctuations within the cavity, porous walls were separately placed at the forward bulkhead, floor, and aft bulkhead. A vent chamber whose pressure was assumed to be uniform was placed behind the porous wall. Numerical experiments showed that replacing the aft bulkhead by a porous wall was most effective for suppressing pressure fluctuations. Small values of porosity ($\sigma = 0.1$) for the porous wall were effective in suppressing pressure oscillation. Increasing the porosity only slightly increased the effectiveness. All the tested values of vent chamber pressure, $p_c = p_\infty$, $1.25p_\infty$, and $1.5p_\infty$, were effective in reducing the sound pressure level, but a high chamber pressure was even more effective.

Acknowledgment

Supported by Grant 82-0424-E006-042 from the National Science Council of Taiwan, Republic of China.

References

[1]Rockwell, D., and Naudascher, E., "Review—Self-Sustaining Oscillations of Flow Past Cavities," *Journal of Fluid Engineering*, Vol. 100, No. 2, 1978, pp. 152–165.

[2]Charwat, A. F., Roos, J. N., Dewey, F. C., Jr., and Hitz, J. A., "An Investigation of Separated Flows—Part I: The Pressure Field," *Journal of Aerospace Sciences*, Vol. 28, No. 6, 1961, pp. 457–470.

[3]Charwat, A. F., Roos, J. N., Dewey, F. C., Jr., and Hitz, J. A., "An Investigation of Separated Flows—Part II: Flow in Cavity and Heat Transfer," *Journal of Aerospace Sciences*, Vol. 28, No. 7, 1961, pp. 513–527.

[4]Tam, C. K. W., and Block, P. J. W., "On the Tones and Pressure Oscillations Induced by Flow over Rectangular Cavities," *Journal of Fluid Mechanics*, Vol. 89, Pt. 2, 1978, pp. 373–399.

[5]Komerath, N. M., Ahuja, K. K., and Chambers, F. W., "Prediction and Measurement of Flow over Cavities—A Survey," AIAA Paper 87-0166, Jan. 1987.

[6]Srinivasan, S., "Numerical Simulation of Turbulent Three-Dimensional Cavity Flow," Ph.D. Dissertation, Old Dominion Univ., Norfolk, VA, Aug. 1988.

[7]Plentovich, E. B., Stallings, R. L., and Tracy, M. B., "Experimental Cavity Pressure Measurements at Subsonic and Transonic Speeds. Static-Pressure Results," NASA Langley Research Center, NASA-TP-3358, Hampton, VA, Dec. 1993.

[8]Atwood, C. A., "Computation of a Controlled Store Separation from a Cavity," AIAA Paper 94-0031, Jan. 1994.

[9]Rossiter, J. E., "Wind Tunnel Experiments on the Flow over Rectangular Cavities at Subsonic and Transonic Speeds," British Aeronautical Research Council, RM 3438, Oct. 1964.

[10]Hankey, W. L., and Shang, J. S., "Analyses of Pressure Oscillations in an Open Cavity," *AIAA Journal*, Vol. 18, No. 8, 1980, pp. 892–898.

[11]Heller, H. H., and Bliss, D. B., "Aerodynamically Induced Pressure Oscillations in Cavities—Physical Mechanisms & Suppression Concepts," AFFDL-TR-74-133, Aug. 1974.

[12]Franke, M. E., and Carr, D. L., "Effect of Geometry on Open Cavity Flow-Induced Pressure Oscillations," AIAA Paper 75-492, March 1975.

[13]Jeng, Y. N., and Wu, T. J., "Numerical Study of a Supersonic Open Cavity Flow with Geometric Modification on Aft Bulkhead," AIAA Paper 92-2627, June 1992.

[14]Sarohia, V., and Massier, P. F., "Control of Cavity Noise," AIAA Paper 76-528, July 1976.

[15]Franke, M. E., and Sarohia, R. E., "Suppression of Flow-Induced Pressure Oscillations in Cavities," AIAA Paper 90-4018, Oct. 1990.

[16]Kim, I., and Chokani, N., "Navier-Stokes Simulations of Unsteady Supersonic Cavity Flowfield with Passive Control," *Journal of Aircraft*, Vol. 29, No. 2, 1992, pp. 217–223.

[17]Chokani, N., and Kim, I., "Suppression of Pressure Oscillation in an Open Cavity by Passive Pneumatic Control," AIAA Paper 91-1729, June 1991.

[18]Borland, C. J., "Numerical Prediction of the Unsteady Flowfield in an Open Cavity," AIAA Paper 77-673, June 1977.

[19]Hankey, W. L., and Shang, J. S., "Analysis of Pressure Oscillations in an Open Cavity," *AIAA Journal*, Vol. 18, No. 8, 1980, pp. 892–898.

[20]Gorski, J. J., Ota, D. K., and Chakravarthy, S. R., "Calculations

of Three-Dimensional Cavity Flow Fields," AIAA Paper 87-0117, Jan. 1987.

[21]Baysal, O., and Stallings, R. L., Jr., "Computational and Experimental Investigation of Cavity Flowfields," *AIAA Journal*, Vol. 26, No. 1, 1988, pp. 6, 7.

[22]Baysal, O., and Srinivasan, S., "Unsteady Viscous Calculations of Supersonic Flows Past Deep and Shallow Three-Dimensional Cavities," AIAA Paper 88-0101, Jan. 1988.

[23]Rizzetta, D. P., "Numerical Simulation of Supersonic Flow over a Three-Dimensional Cavity," *AIAA Journal*, Vol. 26, No. 7, 1988, pp. 799–807.

[24]Zhang, X., and Edwards, J. A., "Computational Analysis of Unsteady Supersonic Cavity Flows Driven by Thick Shear Layers," *The Aeronautical Journal*, Vol. 92, No. 919, 1988, pp. 365–374.

[25]Zhang, X., and Edwards, J. A., "An Investigation of Supersonic Oscillatory Cavity Flows Driven by Thick Shear Layers," *The Aeronautical Journal*, Vol. 94, No. 940, 1990, pp. 355–364.

[26]Baysal, O., "Supercomputing of Supersonic Flows Using Upwind Relaxation and MacCormack Schemes," *Journal of Fluid Engineering*, Vol. 110, No. 1, 1988, pp. 62–68.

[27]Srinivasan, S., "Navier-Stokes Calculations of Transonic Flows Past Cavities," *Journal of Fluid Engineering*, Vol. 113, Sept. 1991, pp. 368–376.

[28]Fouladi, K., and Baysal, O., "Viscous Simulation Method for Unsteady Flows Past Multicomponent Configurations," *Journal of Fluid Engineering*, Vol. 114, June 1992, pp. 161–169.

[29]Baysal, O., Fouladi, K., Leung, R. W., and Sheftic, J. S., "Interference Flows Past Cylinder-Fin-Sting-Cavity Assemblies," *Journal of Aircraft*, Vol. 29, No. 2, 1992, pp. 194–202.

[30]Coakley, T. J., "Implicit Upwind Methods for the Compressible Navier-Stokes Equations," AIAA Paper 83-1958, July 1983.

[31]Payne, U. J., "Modifications on TVD Schemes and the Application to Unsteady Supersonic Open Cavity Flow with/Without the Suppression of Pressure Fluctuations," Ph.D. Dissertation, Inst. of Aeronautics and Astronautics, National Cheng Kung Univ., Tainan, Taiwan, ROC, 1992.

[32]Jeng, Y. N., Payne, U. J., and Wu, T. J., "On the Improvement of TVD Schemes by an Adaptive Limiter and an Extremum Discriminator," *Proceedings of the 8th National Conference of the Chinese Society of Mechanical Engineering* (Taipei, Taiwan, ROC), 1991, p. 103.

[33]Leonard, B. P., and Niknafs, H. S., "Sharp Monotonic Resolution of Discontinuities Without Clipping of Narrow Extrema," *Computers and Fluids*, Vol. 19, No. 1, 1991, pp. 141–154.

[34]Roe, P. L., "Approximate Riemann Solvers, Parameter Vectors, and Difference Schemes," *Journal of Computational Physics*, Vol. 43, No. 2, 1981, pp. 357–372.

[35]Chakravarthy, S. R., and Osher, S., "A New Class of High Accuracy TVD Schemes for Hyperbolic Conservation Laws," AIAA Paper 85-0363, Jan. 1985.

[36]Baldwin, B. S., and Lomax, H., "Thin Layer Approximations and Algebraic Model for Separated Turbulent Flows," AIAA Paper 78-257, Jan. 1978.

[37]Yee, H. C., and Harten, A., "Implicit TVD Schemes for Hyperbolic Conservation Laws in Curvilinear Coordinates," *AIAA Journal*, Vol. 25, No. 2, 1987, pp. 266–274.

[38]Beam, R. M., and Warming, R. F., "An Implicit Factored Scheme for the Compressible Navier-Stokes Equations," *AIAA Journal*, Vol. 16, No. 4, 1978, pp. 393–402.

[39]Pulliam, T. H., "Euler and Thin Layer Navier-Stokes Codes: ARC2D, ARC3D," *Computational Fluid Dynamics*, Workshop at the Univ. of Tennessee Space Inst., Tullahoma, TN, March 1984, pp. 15.1–15.85.

[40]Musker, A., "Explicit Expression for the Smooth Wall Velocity Distribution in a Turbulent Boundary Layer," *AIAA Journal*, Vol. 17, No. 6, 1979, pp. 655–657.

[41]Glimm, J., "Solutions in the Large for Nonlinear Hyperbolic Systems of Equations," *Communications on Pure and Applied Mathematics*, Vol. 18, 1965, pp. 697–715.

[42]Zhang, X., "An Experimental and Computational Investigation into Supersonic Shear Layer Driven Single and Multiple Cavity Flows," Ph.D. Dissertation, Dept. of Engineering, Univ. of Cambridge, Cambridge, England, UK, 1987.

[43]Wilcox, F. J., "Experimental Investigation of Porous-Floor Effects on Cavity Flow Fields at Supersonic Speeds," NASA Langley Research Center, NASA-TP-3032, Hampton, VA, Nov. 1990.